AD-A142 872 CREEP-FATIGUE INTERACTIONS IN ADVANCED EUTECTIC SOPERALLOYS(U) RENSSELAERPPOLYTECHNIC INST TROY NY DEPT OF MATERIALS ENGINEERING K N JONES ET AL. 20 APR 84 1/1

UNCLASSIFIED AFOSR-TR-84-0531 AFOSR-80-0015 F/G 20/11 NL

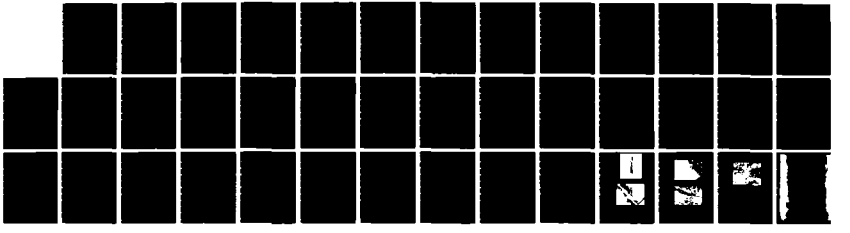

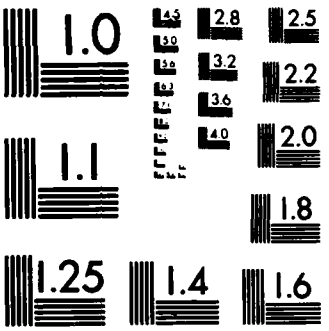

AD-A142 872

UNCLASSIFIED
SECURITY CLASSIFICATION

(13)

REPORT DOCUMENTATION PAGE

1a. REPORT SECURITY CLASSIFICATION Unclassified	1b. RESTRICTIVE MARKINGS
2a. SECURITY CLASSIFICATION AUTHORITY	3. DISTRIBUTION/AVAILABILITY OF REPORT Approved for public release; Distribution unlimited
2b. DECLASSIFICATION/DOWNGRADING SCHEDULE	
4. PERFORMING ORGANIZATION REPORT NUMBER(S)	5. MONITORING ORGANIZATION REPORT NUMBER(S) AFOSR-TR- 84 0531
6a. NAME OF PERFORMING ORGANIZATION Rensselaer Polytech Inst 6b. OFFICE SYMBOL (If applicable)	7a. NAME OF MONITORING ORGANIZATION AFOSR/NE
6c. ADDRESS (City, State and ZIP Code) Rensselaer Polytechnic Institute Troy, N.Y. 12181	7b. ADDRESS (City, State and ZIP Code) Bldg. 410 Bolling AFB, D.C. 20332
8a. NAME OF FUNDING/SPONSORING ORGANIZATION AFOSR 8b. OFFICE SYMBOL (If applicable) NE	9. PROCUREMENT INSTRUMENT IDENTIFICATION NUMBER AFOSR-80-0015
8c. ADDRESS (City, State and ZIP Code) Bldg. 410 Bolling AFB, D.C.	10. SOURCE OF FUNDING NOS. PROGRAM ELEMENT NO. 61102F; PROJECT NO. 2306; TASK NO. A1; WORK UNIT NO.
11. TITLE (Include Security Classification) Creep-Fatigue Interactions in Advanced Eutectic Superalloys	
12. PERSONAL AUTHOR(S) K.N. Jones, N. Bylina, N.S. Stoloff	
13a. TYPE OF REPORT Final 13b. TIME COVERED FROM 1 Oct 79 TO 30 Sep 83	14. DATE OF REPORT (Yr., Mo., Day) April 1984 15. PAGE COUNT 36
16. SUPPLEMENTARY NOTATION	
17. COSATI CODES FIELD / GROUP / SUB GR.	18. SUBJECT TERMS (Continue on reverse if necessary and identify by block number) Superalloys, Creep-Fatigue, D.S. Eutectic

19. ABSTRACT (Continue on reverse if necessary and identify by block number)

Nitac 14B is the most resistant of the three alloys to HCF when all are tested in the as-D.S. condition. AG-170 is the most responsive of the three alloys to an aging heat treatment, due to more effective solutioning and to the precipitation of fine a Mo platelets in the y/y' matrix. Although a sharp drop in HCF resistance occurs in all alloys between 25$_o$C, this decrease may be overcome by an aging treatment, especially for AG-170. Strong creep-fatigue interactions occur in aged Nitac 14B at 825°C. LCF data of Nitac 14B and AG-170 at 800°C obey the Coffin-Manson relation. AG-170 displays superior LCF resistance to Nitac 14B, especially at high plastic strains. Hold times lead to reduced LCF lives, consistent with creep-fatigue effects noted in NCF tests. Limited crack growth data indicate little effect of fiber type or matrix microstructure on crack growth rates. Cracking in y/y'-base eutectics occurs predominantly in stage I at 25°C, with more of a tendency to dimpled rupture in the range 800-825°C.

20. DISTRIBUTION/AVAILABILITY OF ABSTRACT UNCLASSIFIED/UNLIMITED ☐ SAME AS RPT ☐ DTIC USERS ☐	21. ABSTRACT SECURITY CLASSIFICATION Unclassified
22a. NAME OF RESPONSIBLE INDIVIDUAL Dr. Alan H. Rosenstein	22b. TELEPHONE NUMBER (Include Area Code) 202-767-4932 22c. OFFICE SYMBOL NE

DD FORM 1473, 83 APR EDITION OF 1 JAN 73 IS OBSOLETE

SECURITY CLASSIFICATION

AFOSR-TR-

Final Report

to

Air Force Office of Scientific Research

under

Grant No. AFOSR-80-0015

entitled

CREEP-FATIGUE INTERACTIONS IN ADVANCED EUTECTIC SUPERALLOYS

April 20, 1984

by

K.N. Jones, N. Bylina and N.S. Stoloff
Materials Engineering Department
Rensselaer Polytechnic Institute
Troy, NY 12181

Final Report

to

Air Force Office of Scientific Research

under

Grant No. 80-0015

entitled

CREEP-FATIGUE INTERACTIONS IN ADVANCED EUTECTIC SUPERALLOYS

April 20, 1984

by

K.N. Jones, N. Bylina and N.S. Stoloff
Materials Engineering Department
Rensselaer Polytechnic Institute
Troy, NY 12181

INTRODUCTION

This project has been concerned with three facets of cyclic deformation of advanced eutectic composites:

a) high cycle, stress controlled fatigue

b) stress controlled crack growth

c) low cycle, strain controlled fatigue.

Three alloys were selected for study: Nitac 14B, Cotac 744 and AG-170, see Table 1 for nominal compositions. Experiments have been carried out as a function of several variables: temperature, microstructure, and frequency, in order to obtain as complete a picture as possible of the relative advantages and disadvantages of the three alloys under cyclic loading conditions. In addition, the response of these alloys to cyclic deformation has been compared to that of conventional nickel base alloys. Early in the program it was noted that Cotac 744 was inferior in HCF and LCF properties to the other two alloys. Consequently, during the final year of the program LCF and da/dN tests were carried out on AG-170 and Nitac 14B only.

EXPERIMENTAL PROCEDURE

All ingots were melted and directionally solidified at General Electric Co. Solidified rates were 1 cm/hr for AG-170 and 0.635 cm/hr for Nitac 14B and Cotac 744. The ingots were in the shape of right cylinders with diameters of 4.1 cm and 2.2 cm for AG-170 and Nitac 14B, respectively.

The as-received ingots were optically examined along a longitudinal strip polished on the ingot to determine length of integrity and degree of alignment of the microstructure. Transverse sections also were examined to verify that the correct fiber alignment and growth conditions had been obtained.

High Cycle Fatigue

Most ingots contained enough acceptable fibrous structure such that five sections, each 3.8 cm to 4 cm long, could be cut for specimens. Insufficient

aligned structure in other ingots allowed for the cutting of only three or four sections, these being from the center of the ingot. Four right cylinders were electro-discharge machined from each section with the growth direction aligned lengthwise. Specimens were then machined from these cylinders. The diameter of the gage section was 0.254 cm. The overall design of this specimen is shown in Fig. 1.

All specimens were then mechanically polished through 600 grit SiC paper using a high speed tensile lathe. Specimens were examined for non-uniformities, such as deep undercuts, on a stereomicroscope at 70X. This was followed by electropolishing to provide a uniform deformation-free surface. The best electropolish results were obtained using an electrolyte composed of 140 ml methanol, 35 ml H_2SO_4 and 50 ml glycerine cooled with an ice water bath to -10°C. A potential of 32-35 V was applied for 15-30 seconds depending on the alloy. Heat treated specimens were polished differently. The solution was equilibrated at room temperature and a potential of 20 V was applied for 20 seconds. Just prior to testing, the gage diameter of each specimen was measured with a Unitron microscope.

High cycle tests were carried out on an Instron closed loop machine under load control, with a constant minimum stress of 34.5MPa. Threaded split grips were utilized. All tests were conducted under vacuum in a water-cooled chamber. Radiant heating from Kanthal elements produced temperatures to 825°C. The standard test frequency was 20Hz, although a number of tests at 825°C were conducted also at 2, 0.2 and 0.02Hz.

Low Cycle Fatigue

Right cylinders of 0.762 cm diameter were electro-discharge machined from the ingot, parallel to the fiber direction. These cylinders were then turned and ground on a lathe to the final specimen shape. The specimen is a button-end type with a gauge length of 0.635 cm and diameter of 0.33 cm.

All samples were then polished to remove machining grooves. For all samples except the heat-treated AG-170, a mechanical polish on a high speed lathe was used. All samples were polished through 0.3μ Al_2O_3. The heat treated AG-170 were first polished with 600 grit SiC paper to remove the slight oxide and then electro-polished at 5-10°C in a solution of 25% H_2SO_4-75% methanol for 1 minute at 20 volts.

Testing was done on a closed loop servohydraulic MTS machine with a capacity of 10 tons. The specimen was tested in a closed chamber with a dynamic argon environment at 825°C. Specimens were held in the pullrods by a threaded split-grip arrangement. All tests were performed in total axial strain control, at a frequency of 0.2Hz (12 cpm). The cycling was fully reversed (R=-1) with a ramp waveform. Since total strain was controlled, the plastic strain range per cycle changed during the test. Therefore, the plastic strain used in all calculations was measured at $N_f/2$. Hold time tests were performed with a 2 min. hold at the maximum tensile strain.

Crack Growth

Fatigue crack growth rates were measured for two alloys, AG-170 and Nitac 14B, using two different specimen geometries and two different monitoring methods, described below. All tests were performed on the MTS machine described above. Specimens were fatigue loaded using a ramp waveform in load control and a frequency of 20Hz. The R ratio (K_{min}/K_{max}) was kept at 0.05 for all specimens. A simple clevis and pin assembly was used as grips. Room temperature tests were performed in air, while elevated temperature tests were performed in argon. All precracking was done at room temperature. Specimens were tested in the as solidified and heat treated conditions.

Single edge notch (SEN) specimens, measuring 48 mm in length and 20 mm in width with a reduced gauge section thickness of 3.7 mm were used for AG-170.

The samples were oriented such that the fibers were aligned parallel to the loading axis. Samples were electropolished and metallographically inspected to assure a well aligned microstructure and smooth surface. An optical traveling microscope was used to monitor crack growth.

Mini compact tension (CT) specimens with overall width of 26mm, height of 32mm and thickness of 2.9mm. were utilized for Nitac 14B. As for the AG-170 specimens, the fatigue crack was monitored transverse to the growth direction (i.e., fiber length). Specimens were cut from slab-type ingots; interfiber spacing, λ, was 7-10μm and grain diameter averaged 2mm. Samples were metallographically polished and examined. Crack growth was monitored using electropotential drop method verified by optical microscope measurements. A 15 amp DC current was passed through the sample while voltage leads measured the increase in resistance with increasing crack length. A largely linear relationship existed through the life of the specimen, with each millivolt increase in potential signifying a 1mm increase in crack length.

Heat Treatments

Specimens of each type to be heat treated were encapsulated in quartz ampules (1 specimen/ampule). These were evacuated to a pressure of about 0.13Pa. Partial solution treatments for Nitac 14B and Cotac 744 consisted of a 1 hr exposure at 1200°C. AG-170 was solutionized at 1250°C for four hours. All solutionized samples were quenched into iced-brine. Subsequent aging treatments for the three alloys consisted of a 4 hr exposure at 850°C in 0.13Pa vacuum, followed again by an iced-brine quench.

EXPERIMENTAL RESULTS

In each of the following graphs, one data point represents one test, except for FCG data. Scatter noted in the data may be attributed to normal fatigue scatter, slight ingot to ingot variations in microstructure and/or composition, and microstructural defects produced by solidification.

High Cycle Fatigue

Fig. 2 compares HCF properties of three alloys in the as D.S. condition, at 25°C and 825°C. Nitac 14B appeared to be the most fatigue resistant at both temperatures, especially at stress levels well above the fatigue limit. Fatigue resistance declined sharply between 25°C and 825°C. At 825°C, AG-170 is the weakest of the three alloys, displaying a fatigue limit some 20% lower than that of Nitac 14B.

Additional tests on Nitac 14B at constant stress range of 1034MPa resulted in a nearly linear decrease in life with temperature, see Fig. 3.

Heat treatment was found to have a significant effect on the HCF properties of these three alloys, particularly at elevated temperature. A comparison of the room temperature fatigue properties of the three alloys in the aged condition is given in Fig. 4. Nitac 14B is no longer superior; AG-170 exhibits the most improved HCF life of the three after a solutionizing and aging treatment. Nitac 14B and Cotac 744 appear to have comparable lives following this treatment. Fig. 5 compares the results of heat treatment on the elevated temperature fatigue lives of Nitac 14B, Cotac 744 and AG-170. AG-170, previously found to display the worst 825°C fatigue properties in the as-D.S. condition, shows the best S-N properties following aging. However, for fatigue lives exceeding 5×10^6 cycles, Nitac 14B is superior; Cotac 744 reveals the lowest fatigue resistance.

Fig. 6 shows that aging has improved the elevated temperature fatigue resistance of AG-170 more than two orders of magnitude. The room temperature, as-D.S. curve has been included for comparison. Comparing this curve with the 825°C plot for partially solutionized and aged material demonstrates clearly the beneficial effect of heat treatment for HCF resistance at 825°C.

Fig. 7 shows the effects of frequency on aged Nitac 14B at 825°C in vacuum. Reducing the test frequency from 20Hz to 2Hz caused little change in fatigue

life. However, a pronounced influence of test frequency on the S-N curve is noted at lower frequencies. Decreasing the frequency from 2Hz to 0.02Hz produced a reduction in N_f of at least 1000 times at a constant stress. For example, at a stress level of 965MPa the number of cycles to failure decreased from 6×10^6 at 2 Hz to 8.5×10^4 at 0.2Hz and finally to 1.1×10^3 at 0.02Hz.

Additional tests were run on Nitac 14B utilizing two variables: mean stress and surface finish. Both had an effect on the frequency dependence of fatigue life, see Fig. 8a) for cycles to failure vs. N_f and Fig. 8b) for time to failure vs. N_f. Surface finish has a significant effect on cycles or time to failure, Fig. 8, but only at high frequency. This is a reflection of the observation that cracks were surface initiated at high frequency, but originated in the grain interiors at low frequency. It was noted also that fiber damage occurred only adjacent to the primary crack front in samples tested at high frequency, while fibers were damaged throughout the specimen in tests conducted at low frequency.

Although the initial stages of fatigue cracking were thought to occur in Stage I (crystallographic) mode in all of the as-D.S. alloys tested at 25°C, the fatigue zones varied in appearance. The fatigue zone was faceted in AG-170, Cotac 744 showed a fatigue zone which was flat with shallow dimples, while the corresponding regions in Nitac 14B were dimpled. As the crack front advanced into the specimen, the mode of cracking changed to Stage II where the crack propagates normal to the tensile axis. The final fracture occured by a tensile overload.

Fracture surfaces at 825°C in each of the as-D.S. alloys showed few differences from those of specimens tested at 25°C. At 825°C, cracks initiating at the surface were only identified unambiguously in Nitac 14B. However, AG-170 revealed signs of surface initiation. Many of the as-D.S.

AG-170 specimens which were fatigue tested at 825°C did not provide useful data due to the presence of dendrites on the fracture surface. Defects in microstructure, i.e., dendrites, were believed to arise from improper solidification techniques.

Nitac 14B and Cotac 744 readily revealed fiber cracks. In AG-170, only one specimen exhibited fiber cracks. The fatigue zones of samples tested at 825°C were similar in appearance to those tested at 25°C. Nitac 14B and Cotac 744 displayed dimpled fatigue zones, as previously noted. AG-170 once again exhibited a faceted fatigue zone. However, at 825°C the fatigue zone occupied a smaller fraction of the fracture surface than was observed at ambient temperature. Overload regions were found over the remainder of each fracture surface.

Low Cycle Fatigue

A summary of LCF test data appears in Table 2. Data for AG-170 at 825°C are shown in Fig. 9. Note that the data for as-D.S. and for aged material can be effectively described by a single scatter band, and that the Coffin-Manson equation:

$$N_f^{\beta}\Delta\varepsilon_p = \text{Constant} \qquad (1)$$

is obeyed. Two min. hold times produced a small drop in LCF life, based either on total or on plastic strain. Note also that René 80, a conventional nickel-base superalloy, displays markedly inferior LCF resistance (at 871°C).

LCF data for as-D.S. Nitac 14B are shown in Fig. 10. Note that a 2 min. hold time seems more detrimental in this alloy. It may be seen also that, based upon $\Delta\varepsilon_p$, the LCF resistance of this alloy at 825°C is little better than that of René 80 at 871°C.

Values of the Coffin-Manson constants β and C are tabulated for the two

alloys in Table 3. The slope β, is markedly reduced by the hold time for AG-170, but is little affected by hold time for Nitac 14B.

Cyclic hardening data at 825°C for aged AG-170 are shown in Fig. 11, and for as D.S. Nitac 14B in Fig. 12a) for 0 hold time and in Fig. 12b) for 2 min. hold time. Little or no cyclic hardening is noted in these alloys under these test conditions.

Crack Growth

AG-170

Fatigue crack growth rates (FCG) are shown in Fig. 13 for aged AG-170 at room temperature and 800°C. Also included in the graph are results from Hoffman et al,[2] on a similar γ/γ'-α alloy, (see Table 1 for composition). Room temperature FCGR for as-solidified material showed much scatter due to excessive crack branching, seen in the micrograph in Fig. 14. All cracking occurred crystallographically (Stage I). The average values of the as-D.S. room temperature data are comparable to the room temperature data of Hoffman, et al[2] (solid line). Room temperature rates for aged AG-170 (open circles) were higher than the rates for as-D.S. material, thus showing the beneficial effect of crack branching on crack growth retardation. Elevated temperature data (solid circles) showed similar growth rates to the room temperature data at low ΔK values, indicating a single threshold value. At higher values of ΔK, there was an approximately five times increase in growth rate. The mode of cracking changed from crystallographic Stage I at room temperature to Stage II at elevated temperature. The 800°C data fell within the 870°C scatter band (dashed lines) reported by Hoffman et al[2].

Nitac 14B

Fatigue crack growth rates are shown in Fig. 15 for both as D.S. and heat treated Nitac 14B at 25°C and at 800°C. There was little effect of γ' refinement

on fatigue growth rates at both temperatures. Similar to AG-170, there was a five fold increase in FCGR for $\Delta K \geq 20 MPam^{1/2}$ at 800°C and what may appear as overlapping rates at lower ΔK values. The macrograph of Fig. 16 shows that there were four distinct regions of the fracture surface at 25°C. The heat treated and as-D.S. sample appeared almost identical. Crystallographic Stage I cracking, seen in Fig. 17, occurred from initiation until $\Delta K = 17 MPam^{1/2}$. The mode then changed to Stage II (Fig. 18) which itself showed two regions. The initial region was relatively flat (i.e., perpendicular to load axis) and fibrous until $\Delta K \simeq 26 MPam^{1/2}$. The fracture appeared so flat and featureless under low magnification viewing that by tilting the sample, individual grains could be discerned, similar to a polished and not necessarily etched metallographic section. The fracture then appeared more feathery and textured, see Fig. 19, until $\Delta K \simeq 73 MPam^{1/2}$. The final overload region was relatively flat with some delaminated grain boundaries. The elevated temperature samples displayed only Stage II crack growth, appearing very ductile, see Fig. 20, with no real transition noted as in the samples tested at 25°C. Curiously, in both samples tested at high tempeature, the overall crack path was at approximately 20° to the tensile axis. A shear lip existed in both sets of samples at both temperatures, thus indicating the specimens were not under plane strain conditions. No fiber breakage was observed away from the crack front except in the overload regions, where extensive intersecting matrix slip was observed. Elevated temperature results are compared with Udimet 700 (solid line) at 870°C in air from reference 2. It can be concluded that Nitac 14B has comparable fatigue crack growth resistance to that of conventional superalloys.

DISCUSSION

This investigation has demonstrated significant differences in the fatigue response of the three eutectic alloys studied, depending upon microstructural condition and test method. Certain general trends have been established. Nitac 14B is the most resistant of the three alloys to HCF when tested in the as-D.S. condition at either 25°C or 825°C, as shown in Fig. 2. Fatigue lives drop sharply, however, between these temperatures for the three alloys. When tested in the aged condition, AG-170 displays superior HCF resistance, Figs. 3 and 6, due to the inhibition of crack nucleation in the matrix, which is strengthened by α Mo platelets.[3] The refinement in γ' during solution treatment is complete in AG-170, while it is incomplete in the other two alloys. Therefore the superior response of AG-170 to heat treatment is probably due to a combination of effects. The details of the influence of precipitation on strength and fatigue resistance of γ/γ'-α type alloys have been reported in earlier publications[3-5] generated under this contract. The effect of heat treatment in AG-170 is such as to overcome the loss of HCF strength between 25°C and 825°C, as was shown in Fig. 6. Nitac 14B is somewhat less responsive to heat treatment, while Cotac 744 reveals little improvement in LCF properties in the aged condition. The lack of response of Cotac 744 to heat treatment caused us to drop this alloy crack growth portions of the experimental program. Limited LCF data for Cotac 744 resulting from this study have been published.[6]

Another notable feature of the fatigue behavior of Nitac 14B was the significant influence of test frequency on fatigue lives, see Fig. 7. This observation of decreasing life with decreasing frequency in inert environments is consistent with earlier observations on other eutectic alloys.[7,8] The earlier work had led us to conclude that creep-fatigue interactions in eutectic composites are extremely significant at elevated temperatures. Our most recent work, Figs. 8a) and 8b) demonstrated that frequency effects are dependent upon

the surface condition of Nitac 14B. It appears that surface crack initiation occurs during tests at 20Hz, while cracks initiate in the interior of the specimen at lower frequencies. There may be a small affect of R ratio also on frequency-dependence of HCF lives, Fig. 8, but this has not been established with certainty. Creep effects at low frequencies also are manifested in other respects; for example, dislocation penetration of large γ' rosettes is noted at low test frequencies, but not at 20 Hz[10]. Finally, increased cracking of fibers away from the primary crack is noted as frequency is decreased. The preponderance of evidence suggests, therefore, that there is a strong creep-fatigue interaction in these alloys, especially at low test frequencies.

LCF data for Nitac 14B and AG-170 obeyed the Coffin-Manson relation, Eq. 1. AG-170 demonstrated superior LCF lives, especially at low plastic strains. Limited data show that both alloys suffer a loss in LCF life with a 2 min. hold time, see Figs. 9 and 10. The effect is more significant in Nitac 14B. Little or no cyclic hardening was observed in either alloy at 825°C, see Figs. 11 and 12.

Only limited success was achieved in crack growth testing of AG-170 and Nitac 14B. Considerable difficulty was encountered in driving a crack across the specimen with either alloy, due to a strong tendency for crack branching. Nevertheless, increased crack growth rates have been observed in both alloys with rise in temperature from 25°C to 800°C. This increase was observed, however, only above a critical stress intensity range. At low ΔK, there appeared to be little effect of temperature on FCGR. In addition, we have observed little difference in crack growth rates between aged and as-D.S. specimens of the two alloys at either temperature, see Figs. 13 and 15. This observation is consistent with earlier work in which it was concluded that the nature of the fibers has little effect on crack growth in nickel-base γ/γ' matrices.[4] There was little or no effect of aging on crack growth at any ΔK level in Nitac 14B, Fig. 15. The lack of improvement in crack growth response extends to the near

threshold region, which may or may not be related to crack initiation. Since we are unable to link aging with improved crack growth behavior, we suggest that improvements in HCF lives with aging in this alloy are due to delayed crack initiation. In general, it may be inferred that the response of eutectic composites to aging is to be found largely in improved HCF resistance, with little influence on LCF lives or FCG behavior.

Detailed metallographic and fractographic investigations of test samples revealed a strong tendency for stage I cracking in the three alloys at 25°C, see Figs. 14, 17 and 18. In both aged and as-D.S. FCG specimens of AG-170, the mode of cracking was entirely crystallographic at 25°C, whereas in Nitac 14B, the mode changed to stage II after an initial stage I region, see Fig. 16. Cooperative shear between the Mo fibers and matrix may enhance Stage I cracking in AG-170. At 800°C, dimpled fracture surfaces were noted in Nitac 14B, as shown in Fig. 20. A tendency for less faceted cracking at elevated temperatures also has been noted in Cotac 744 and AG-170 in earlier work on this contract.[9] Fatigue cracking at 800-825°C tends to initiate internally at low frequencies, and at the specimen surface at high frequency, 20Hz.

Conclusions

1. Nitac 14B is the most resistant of the three alloys to HCF when all are tested in the as-D.S. condition.
2. AG-170 is the most responsive of the three alloys to an aging heat treatment, due to more effective solutioning and to the precipitation of fine α Mo platelets in the γ/γ' matrix.
3. Although a sharp drop in HCF resistance occurs in all alloys between 25°C and 825°C, this decrease may be overcome by an aging treatment, especially for AG-170.
4. Strong creep-fatigue interactions occur in aged Nitac 14B at 825°C.

5. LCF data of Nitac 14B and AG-170 at 800°C obey the Coffin-Manson relation.

6. AG-170 displays superior LCF resistance to Nitac 14B, especially at high plastic strains.

7. Hold times lead to reduced LCF lives, consistent with creep-fatigue effects noted in HCF tests.

8. Limited crack growth data indicate little effect of fiber type or matrix microstructure on crack growth rates.

9. Cracking in γ/γ'-base eutectics occurs predominantly in stage I at 25°C, with more of a tendency to dimpled rupture in the range 800-825°C.

Publications

The following publications have resulted from this contract:

J.M. Tartaglia and N.S. Stoloff, "Mechanical Effects on High Cycle Fatigue of Ni-Al-Mo Aligned Eutectics", Met. Trans. A, V. 12A, 1981, pp. 1119-1125.

J.M. Tartaglia and N.S. Stoloff, "Fatigue of Ni-Al-Mo Aligned Eutectics at Elevated Temperatures", Met. Trans. A, V. 12A, 1981, pp. 1891-1898.

T. Ishii, D.J. Duquette and N.S. Stoloff, "Microstructure and Mechanical Properties of a Ni-Al-Mo Eutectic Composite", Acta Met., V. 29, 1981, pp. 1467-1472.

K.A. Dannemann, N.S. Stoloff and D.J. Duquette, "The Influence of Microstructure on High Cycle Fatigue of Three Aligned Eutectics in Deformation of Multi-Phase and Particle-Containing Materials", Proc. Fourth RISO Conf., 1983, pp. 205-210.

T. Ishii, D.J. Duquette, and N.S. Stoloff, "The Low Cycle Fatigue Behavior of Three Advanced Nickel-Base Eutectic Composites", in InSitu Composites IV, North Holland, New York, 1982, pp. 59-67.

K.A. Dannemann, T. Ishii, D.J. Duquette and N.S. Stoloff, "Microstructure and Fatigue Behavior of Nickel-Base Eutectic Composites", in Strength of Metals and Alloys, ICSMA 6, V. 1, Peragmon, Oxford, 1982, pp. 141-146.

N.S. Stoloff "The Role of Refractory Metals in High Temperature Aligned Eutectics", in Refractory Alloying Elements in Superalloys, ASM, Metals Park, 1984, pp. 87-100.

In addition, the following manuscripts are in preparation:

K.N. Jones, D.J. Duquette and N.S. Stoloff, "Fatigue Crack Growth in Two Nickel-Base Aligned Eutectics", to be sumbitted to Scripta Met.

N. Bylina, D.J. Duquette and N.S. Stoloff, "Effects of Hold Times on Low Cycle Fatigue of Two Nickel-Base Aligned Eutectics" to be submitted to Scripta Met.

E. Blank, K.A. Dannemann and N.S. Stoloff, "Frequency Effects on Fatigue of a TaC-reinforced Eutectic Composite", to be submitted to Met. Trans. A.

Degrees Granted

The following students, with graduate degrees achieved, have been supported under this Contract:

J. M. Tartaglia, Ph.D.

K. A. Dannemann, M.S.

K. N. Jones, M.S. (to be awarded summer, 1984)

N. Bylina, M.S. (to be awarded summer, 1984).

Other Personnel

The following post-doctoral research associates have participated in this program. Both have returned to the faculties of their institutions, listed below.

T. Ishii, Associate Professor, Misei Univ., Tokyo, Japan

E. Blank, Ecole Polytechnique Federale de Lausanne, Switzerland

References

1. S. D. Antolovich, S. Liu, and R. Baur, Metallurgical Transactions A, 1981, Vol. 12A, p. 473.

2. C. Hoffman, P. Bhowal, and A.J. McEvily, "Fatigue Crack Growth in Co and Ni Base Directionally Solidified Eutectic Composites", In Situ Composites IV, F. Lemkey, H.E. Cline, M. Mclean, Editors, 1982, Elsevier Science Publishing Co.

3. T. Ishii, D.J. Duquette and N.S. Stoloff, Acta Met, V. 29, 1981, p. 1467.

4. J.M. Tartaglia and N.S. Stoloff, Met. Trans. A, V. 12A, 1981, p. 1119.

5. K. A. Dannemann, N.S. Stoloff and D.J. Duquette, Proc. Fourth RISO Conf., Roskilde, Denmark, 1983, p. 205.

6. T. Ishii, D.J. Duquette and N.S. Stoloff, in In Situ Composites IV, North Holland, New York, 1982, p. 59.

7. J.M. Tartaglia and N.S. Stoloff, Met. Trans. A. V. 12A, 1981, p. 1891.

8. W.A. Johnson and N.S. Stoloff, Met. Trans. A., V. 11A, 1980, p. 307.

9. K.A. Dannemann, M.S. Thesis, Rensselaer Polytechnic Institute, Aug. 1982.

10. E. Blank and N.S. Stoloff, unpublished.

Table 1

Alloy Composition (wt %)

Alloy	Ni	Co	Cr	Mo	W	Re	Al	C	Others
Nitac 14B	62.56	3.93	4.20	3.16	4.52	6.84	5.5	0.27	9.01Ta, 0.01B
AG-170	61.53			29.74		1.2	5.88		1.65V
Cotac 744	63.7	10	4	2	10		6	0.5	3.8Nb
γ'-α*	65			27			8		

* Hoffman et al[2]

Table 2

Low Cycle Fatigue Data at 825°C

Alloy	Hold Time	ε_t%	ε_p%	N_f	Heat Treat
AG-170	---	3.1	0.479	465	Aged
AG-170	---	2.06	0.297	1176	Aged
AG-170	---	1.56	0.156	6279	Aged
AG-170	2 min.	3.65	0.546	91	Aged
AG-170	2 min.	3.18	0.438	258	Aged
AG-170	---	3.56	0.82	54	as-D.S.
AG-170	---	2.82	0.40	550	as-D.S.
AG-170	---	1.99	0.32	1341	as-D.S.
Nitac 14B	---	3.64	0.451	182	as-D.S.
Nitac 14B	---	2.87	0.261	458	as-D.S.
Nitac 14B	---	1.73	0.04	1786	as-D.S.
Nitac 14B	---	7.48	2.10	30	as-D.S.
Nitac 14B	---	2.83	0.14	957	as-D.S.
Nitac 14B	2 min.	3.21	0.72	21	as-D.S.
Nitac 14B	2 min.	3.84	0.65	36	as-D.S.
Nitac 14B	2 min.	2.15	0.14	206	as-D.S.

Table 3

Coffin-Manson Constants

$$N_f^{\beta}\Delta\varepsilon_p = C$$

Alloy	Heat Treatment	Hold Time (min)	β	C
AG-170	Sol'n + Aged	0	0.425	0.063
AG-170	Sol'n + Aged	2	0.212	0.014
AG-170	as-D.S.	0	0.296	0.027
Nitac 14B	as-D.S.	0	.773	0.281
Nitac 14B	as-D.S.	2	0.757	0.082

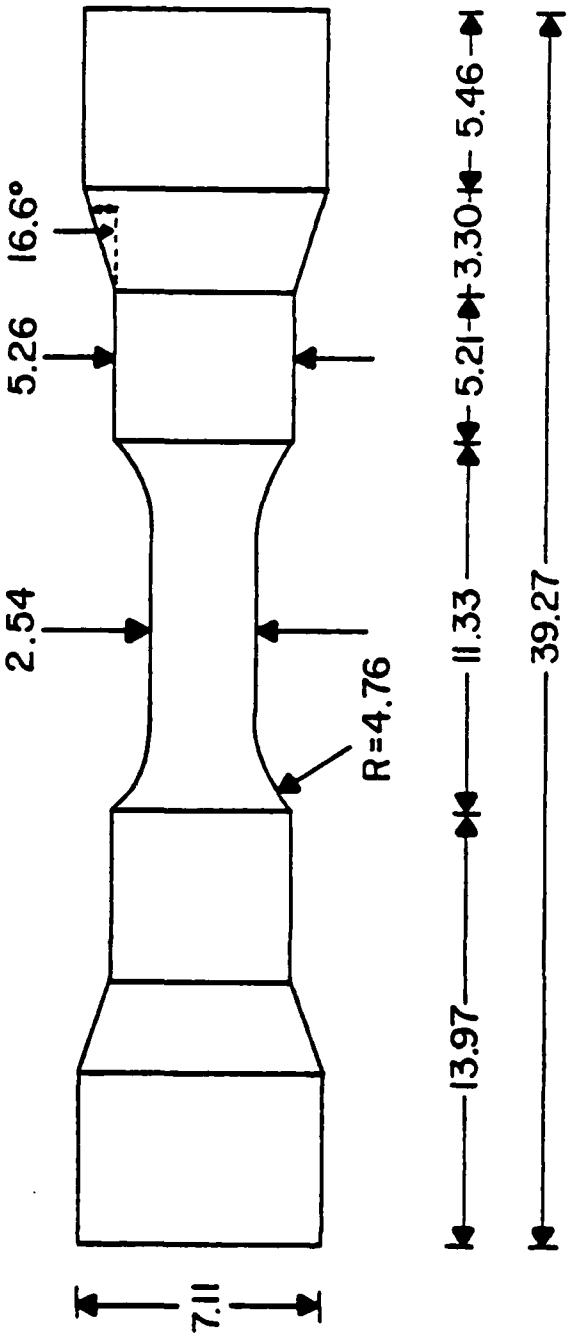

Fig. 1 Fatigue specimen configuration for heat treated material.

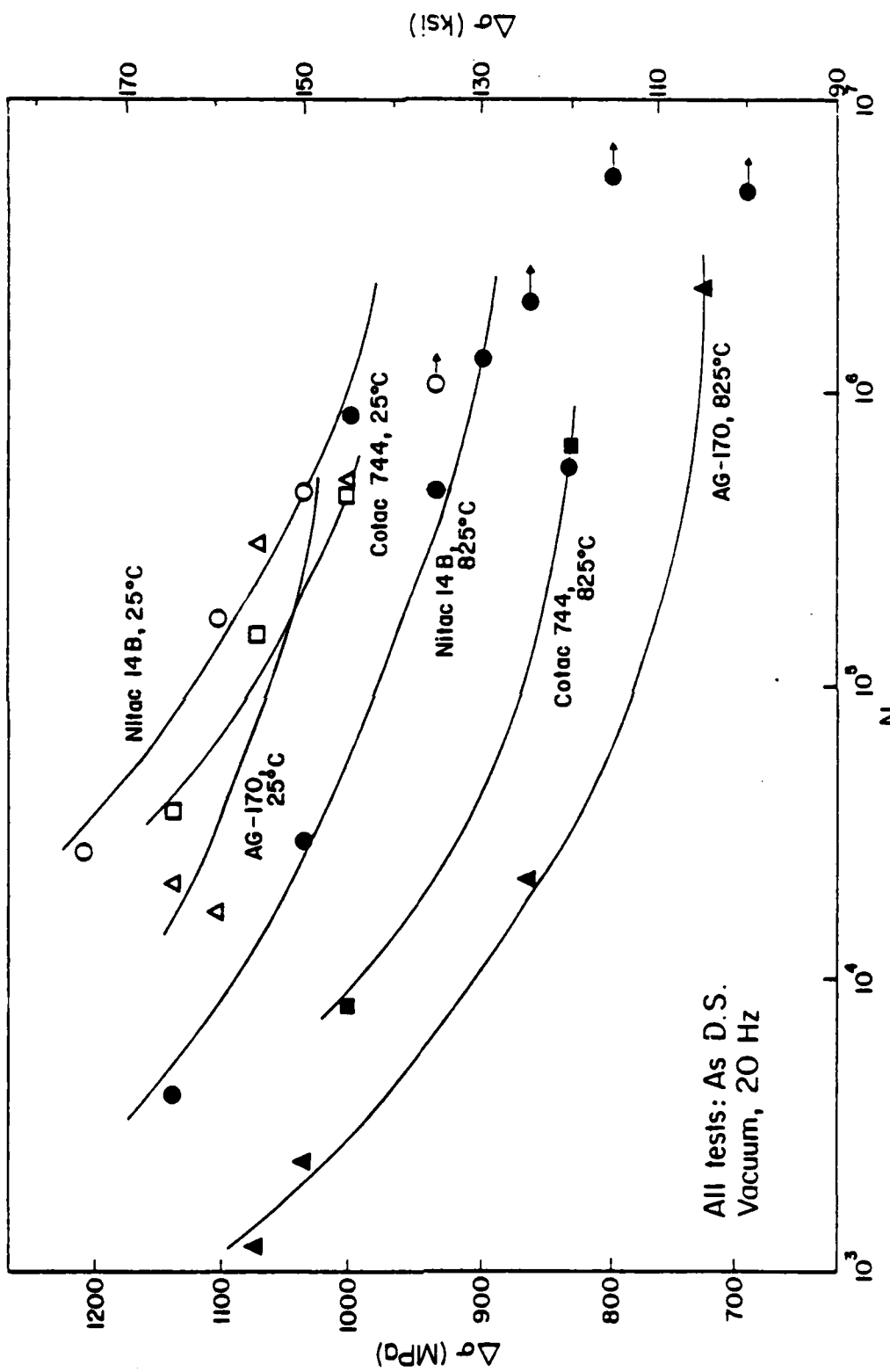

Figure 2 High cycle fatigue properties of the three nickel-base alloys at room temperature and 825°C.

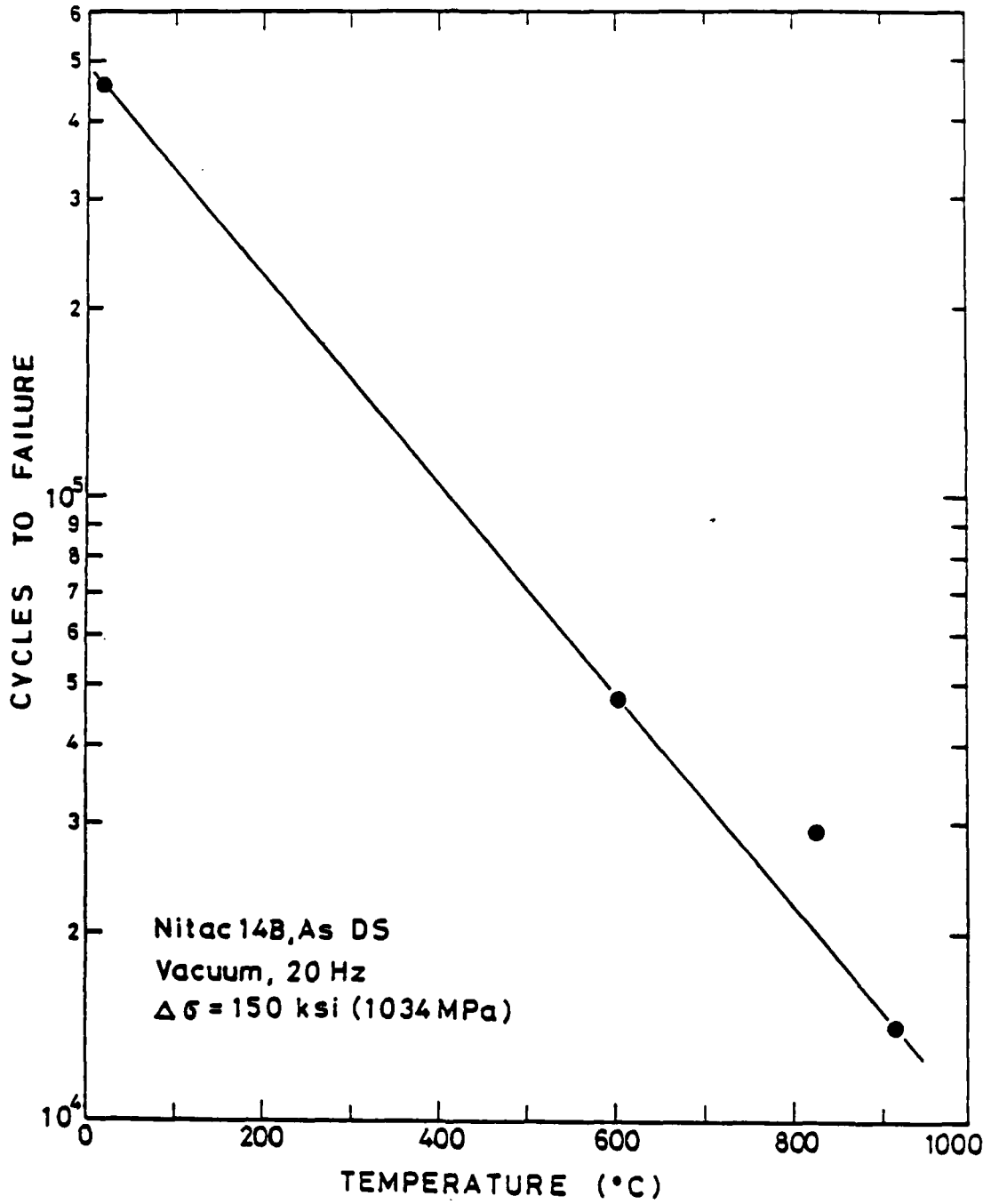

Fig. 3 Effect of temperature on the fatigue life of Nitac 14B at constant $\Delta\sigma$.

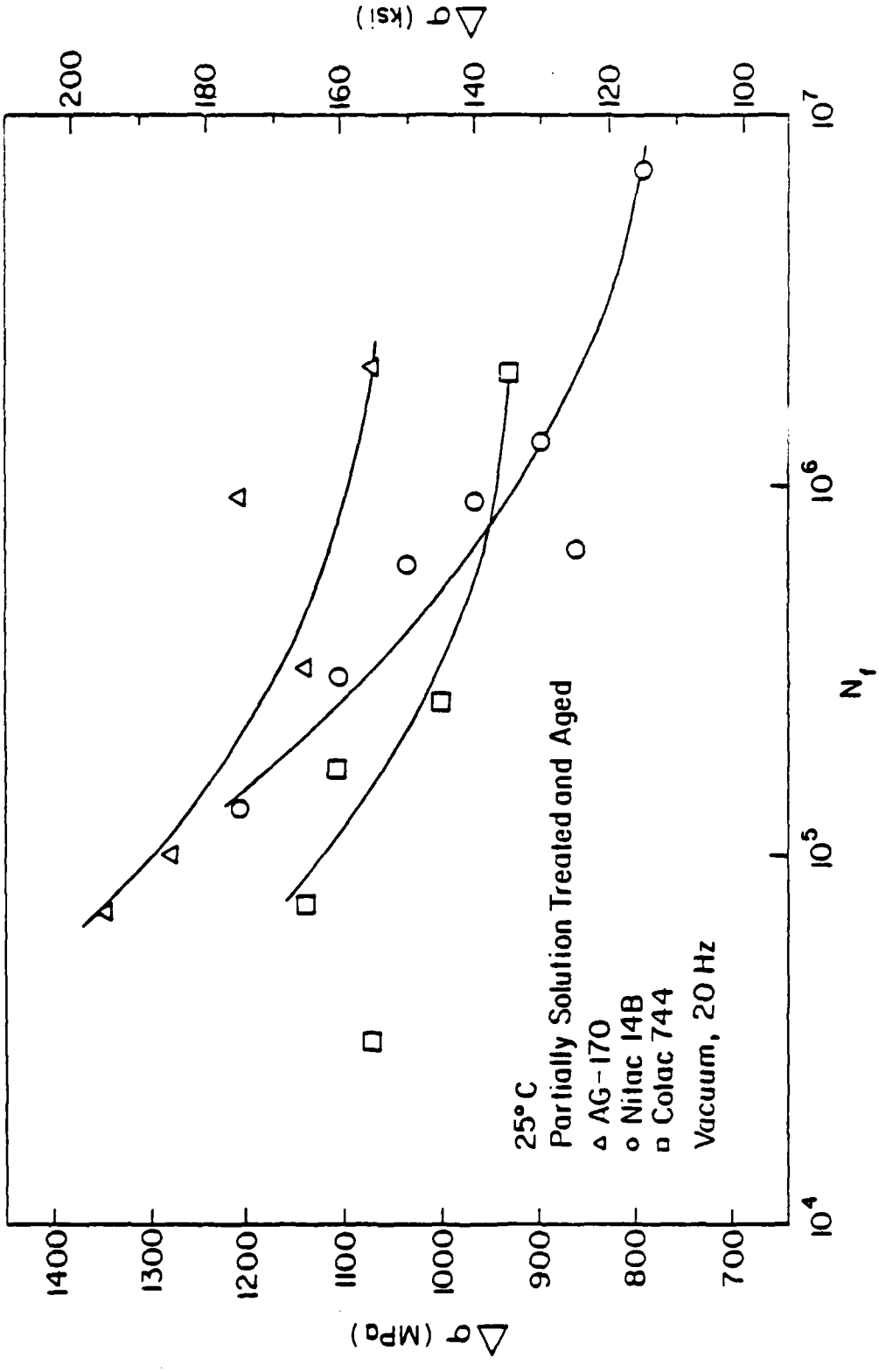

Fig. 4 Effect of heat treatment on the room temperature S-N properties of the three alloys.

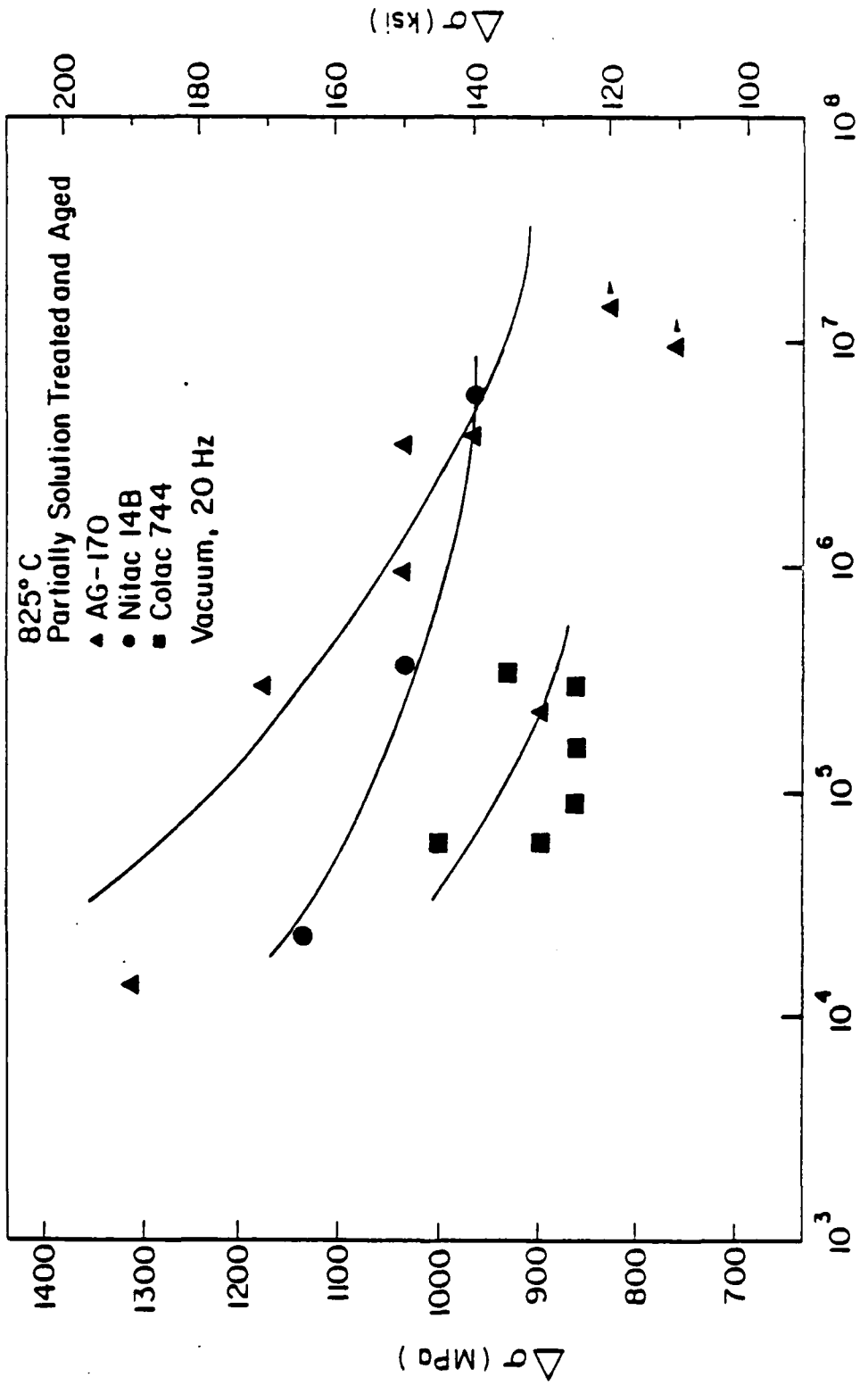

Fig. 5 Effect of heat treatment on the S-N properties of the three eutectics at 825°C.

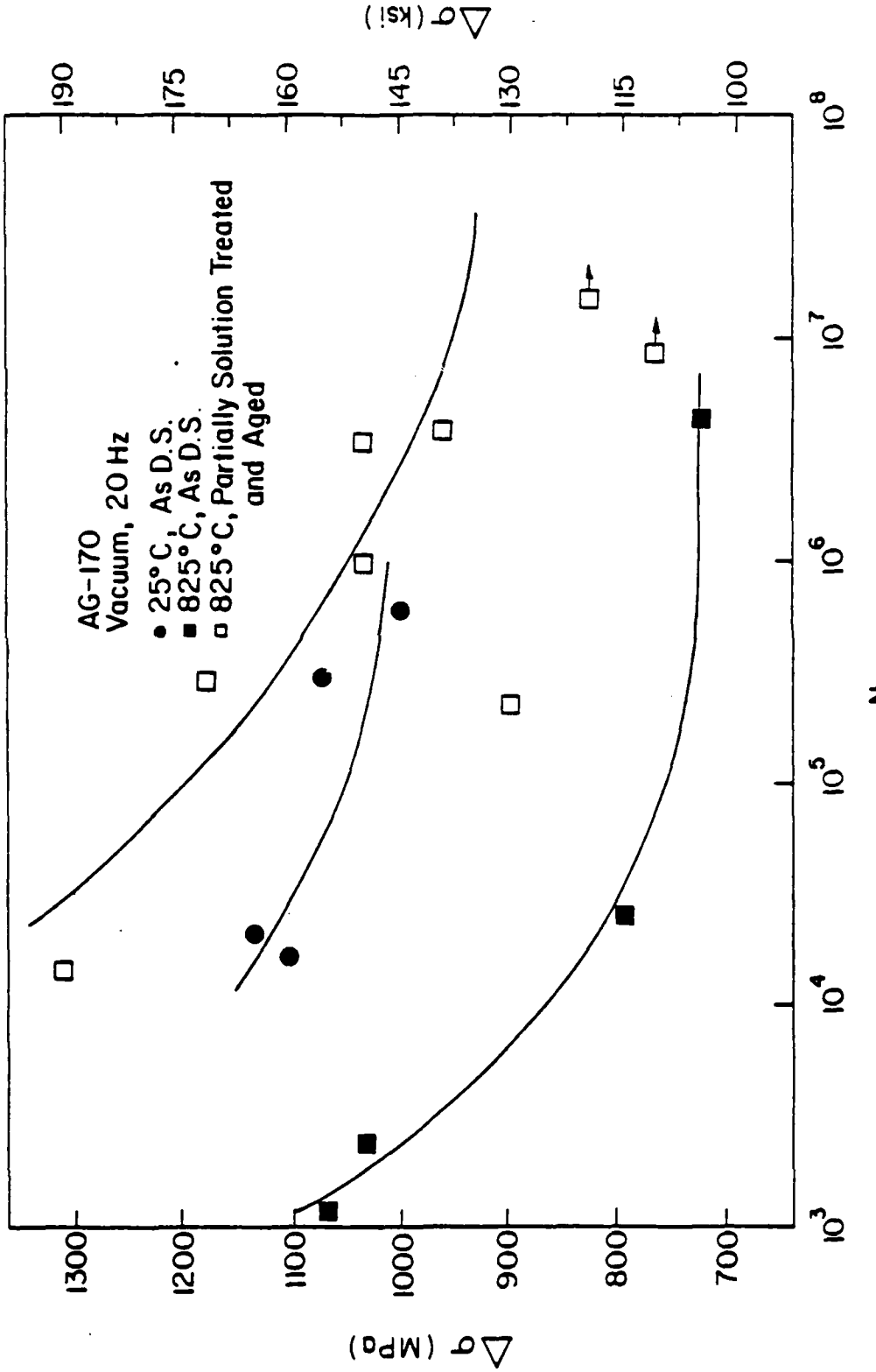

Fig. 6 Effect of aging on the S-N properties of AG-170 at 825°C.

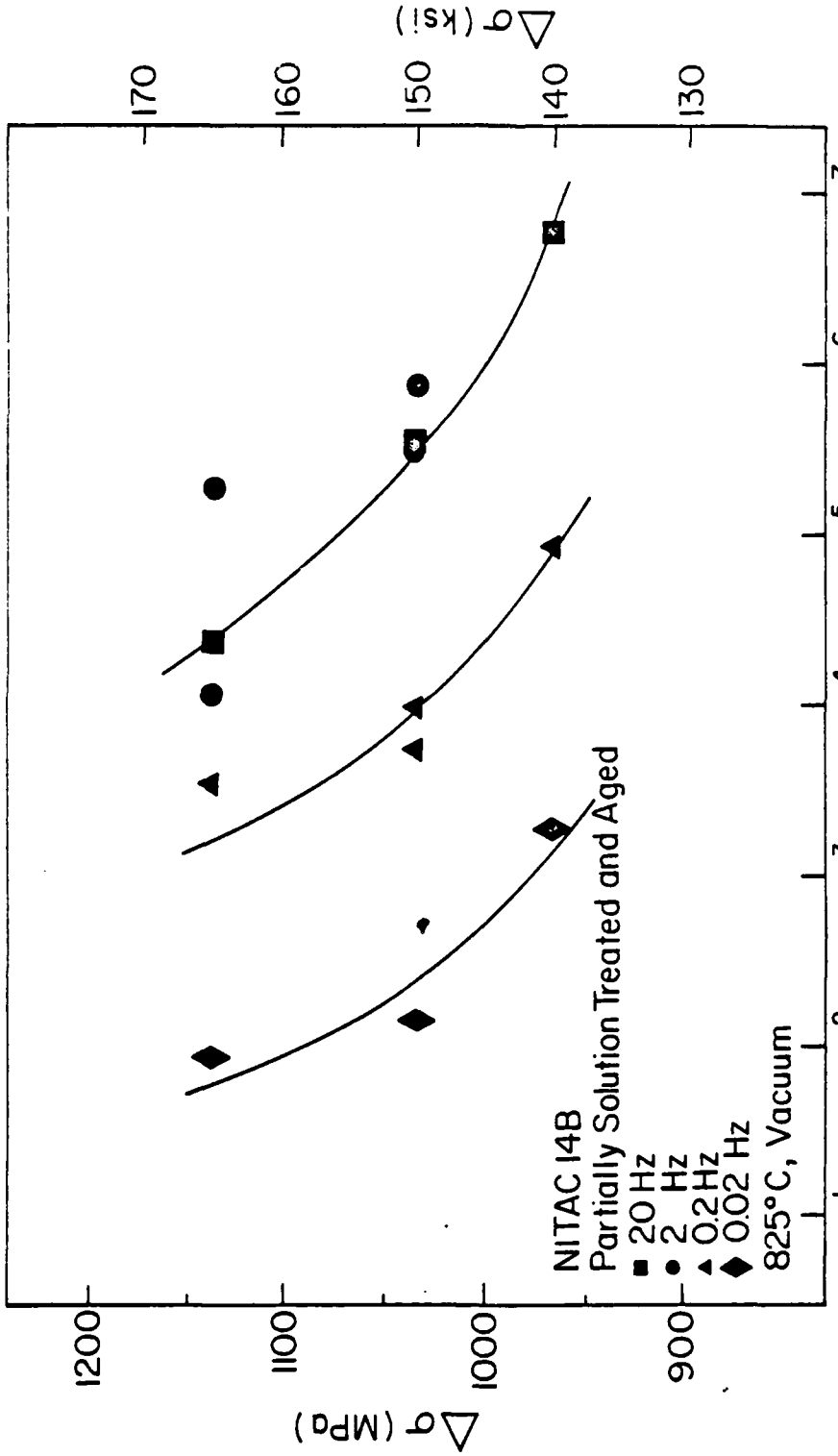

Fig. 7 Effect of frequency on the S-N curve of aged Nitac 14B at 825°C.

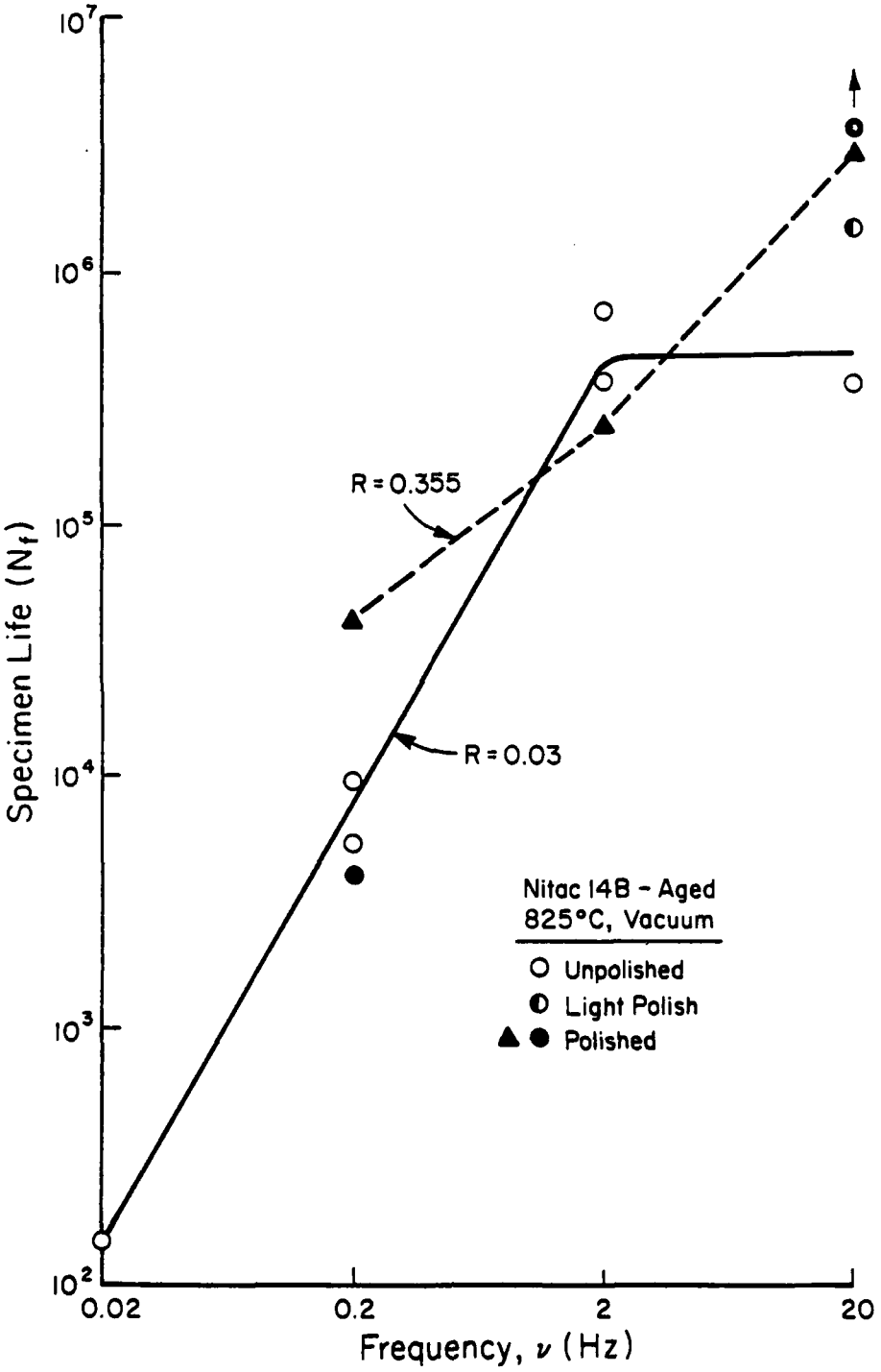

Fig. 8 Fatigue life vs. frequency, Nitac 14B aged, 825°C

a) N_f

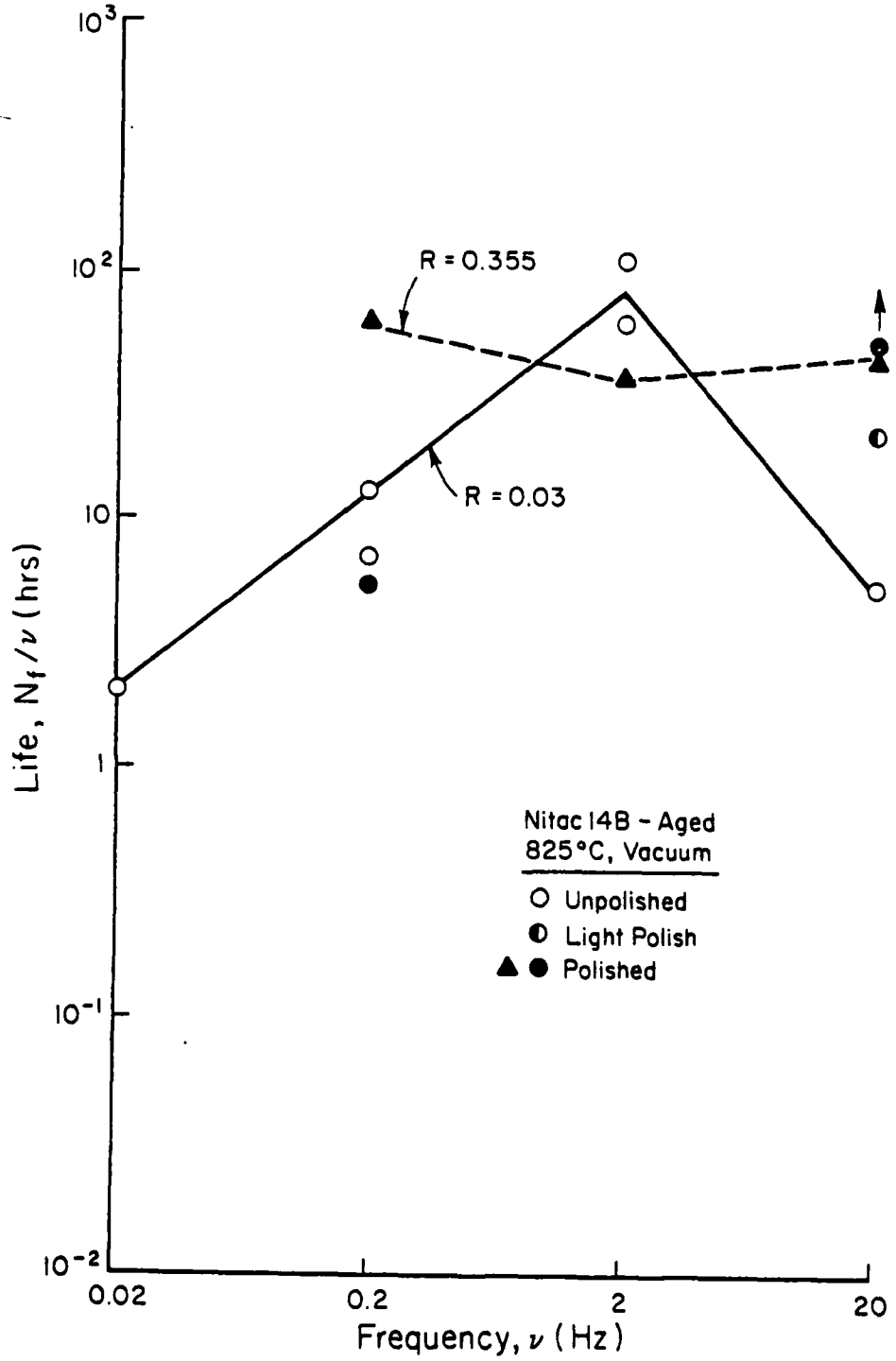

Fig. 8b) $t_F = \frac{N_f}{\nu}$

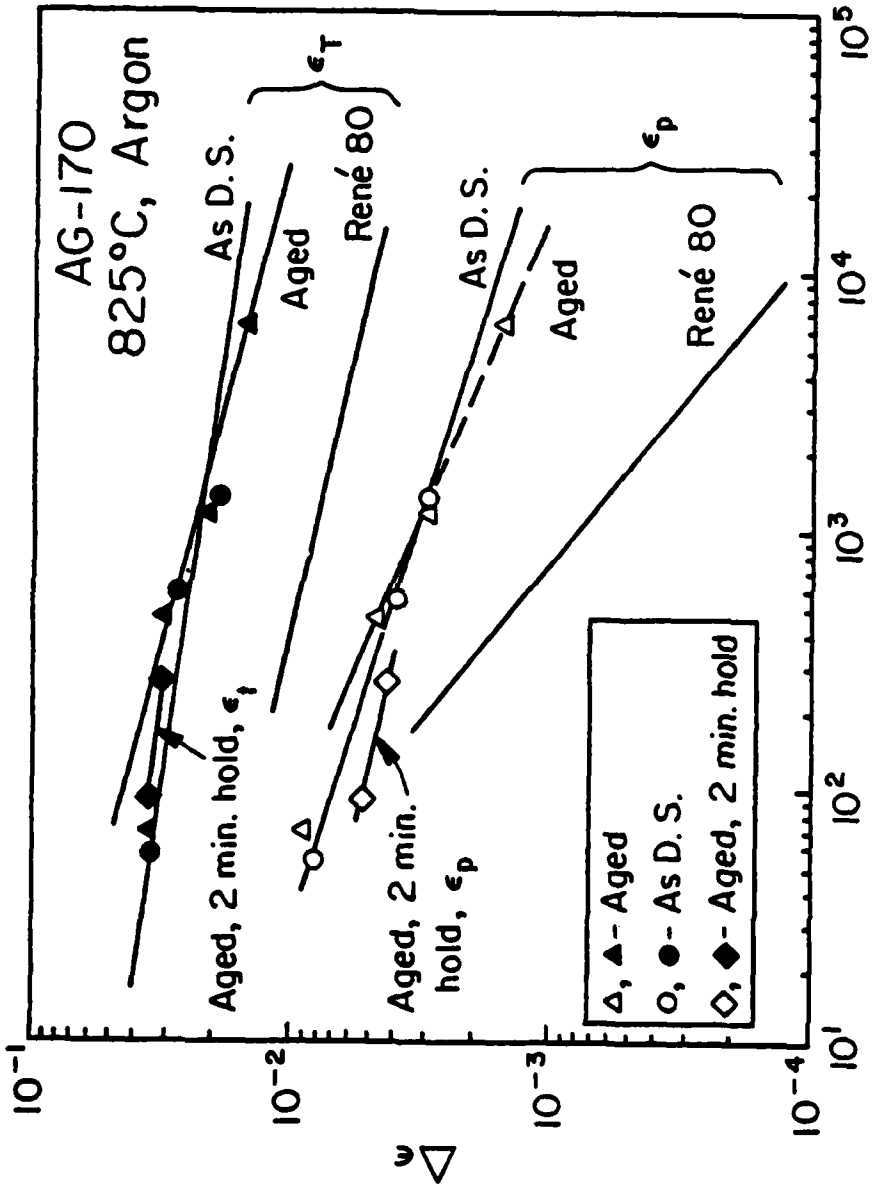

Fig. 9 LCF data for AG-170, 825°C, argon.

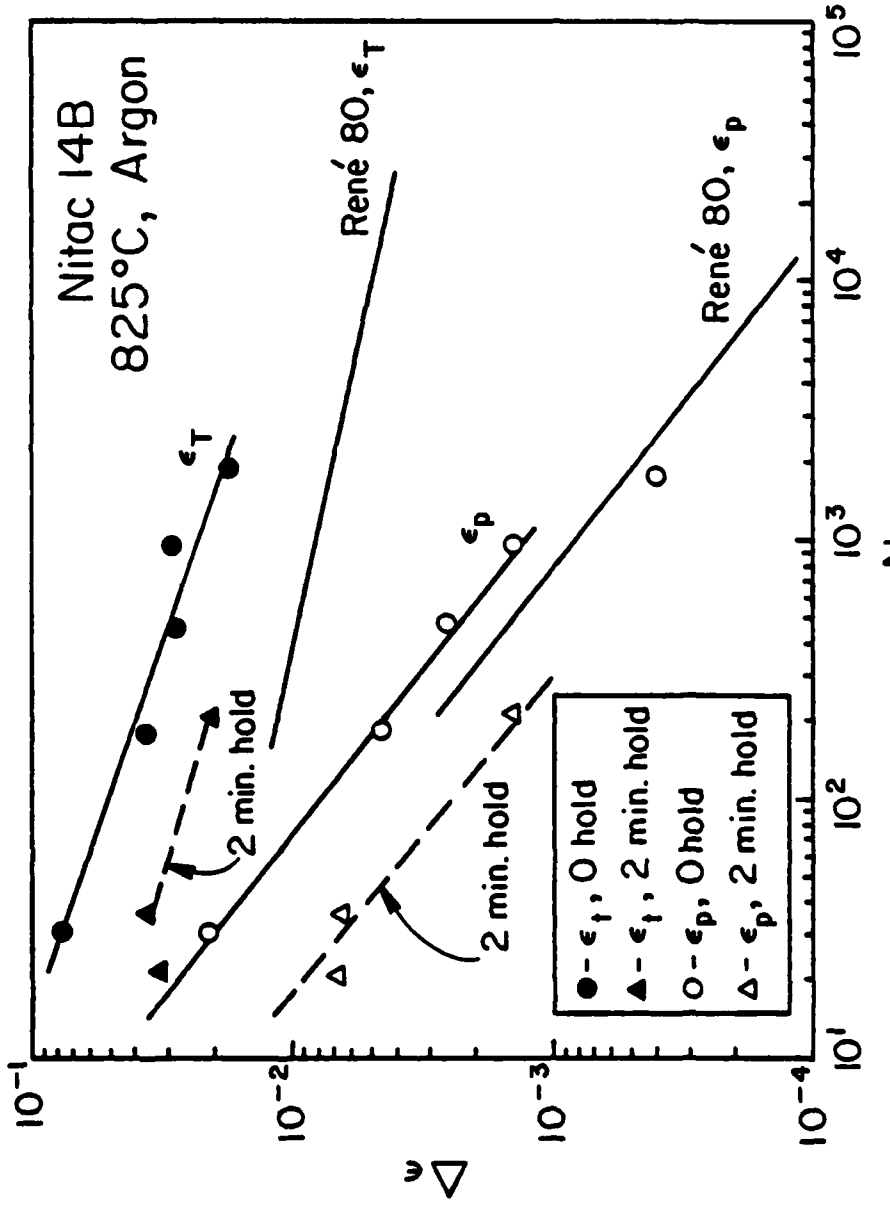

Fig. 10 LCF data for Nitac 14B, 825°C, argon.

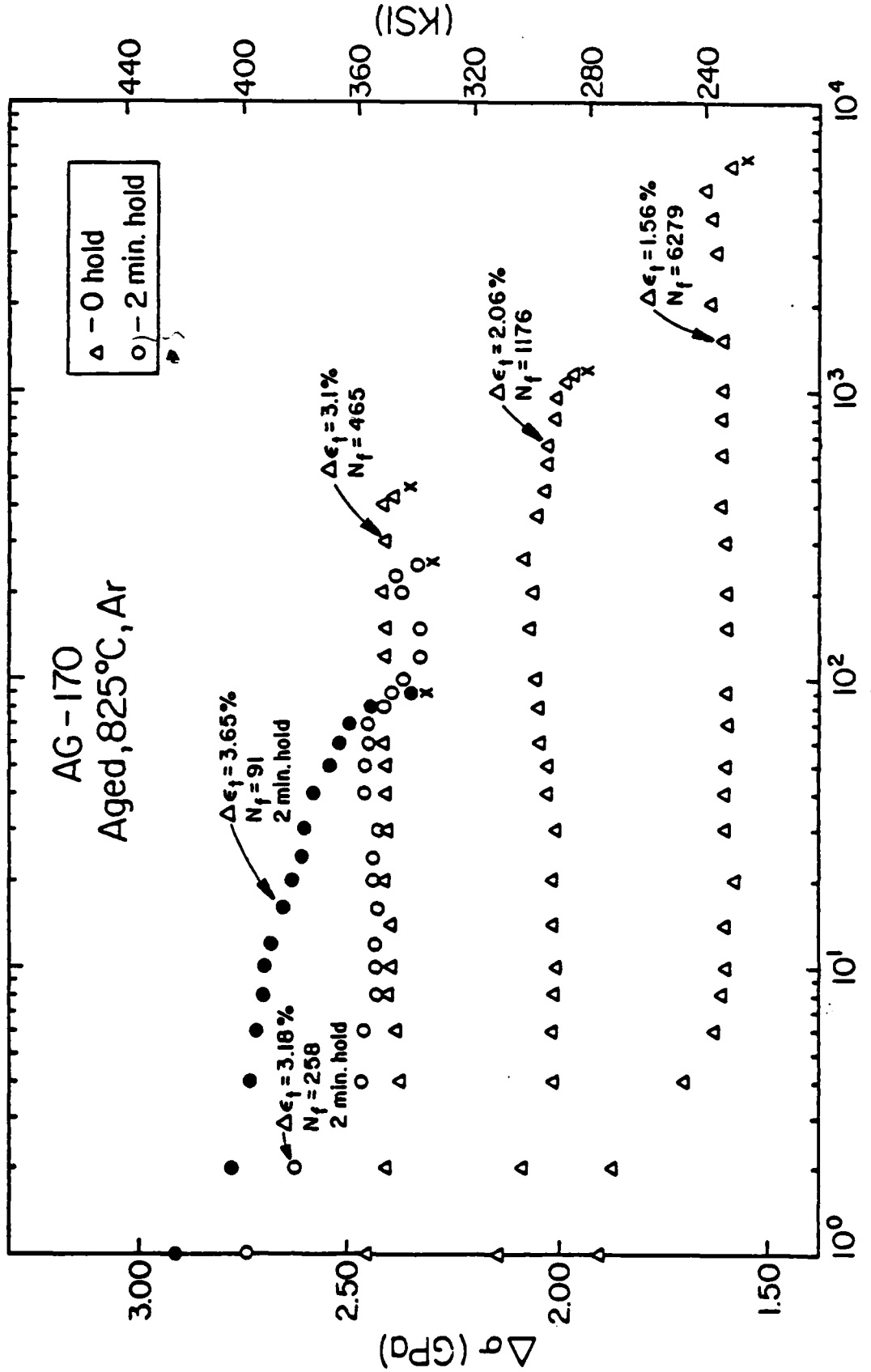

Fig. 11 Cyclic hardening data for AG-170, 825°C, argon.

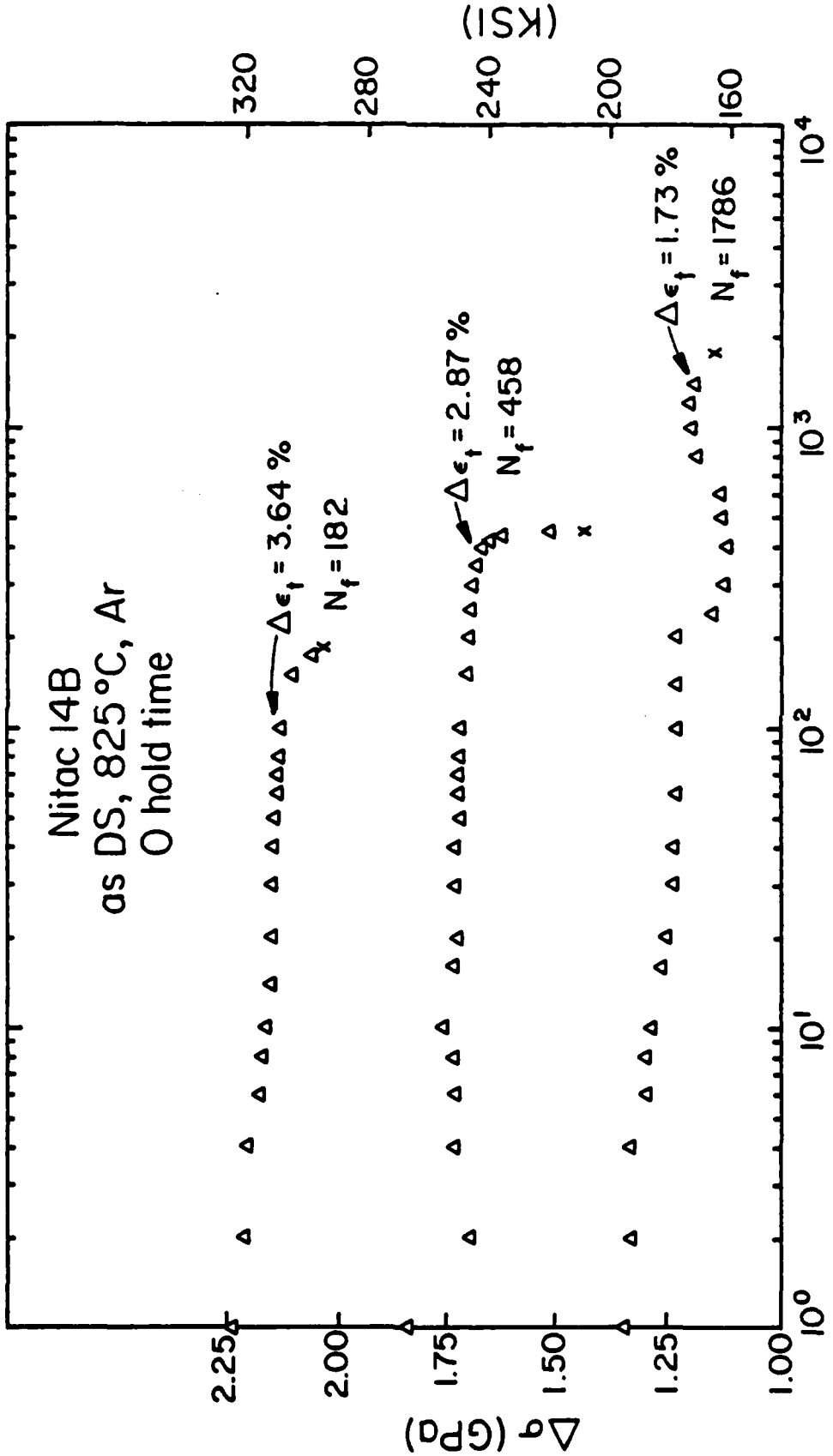

Fig. 12 Cyclic hardening data for Nitac 14B, 825°C, argon

a) 0 hold time

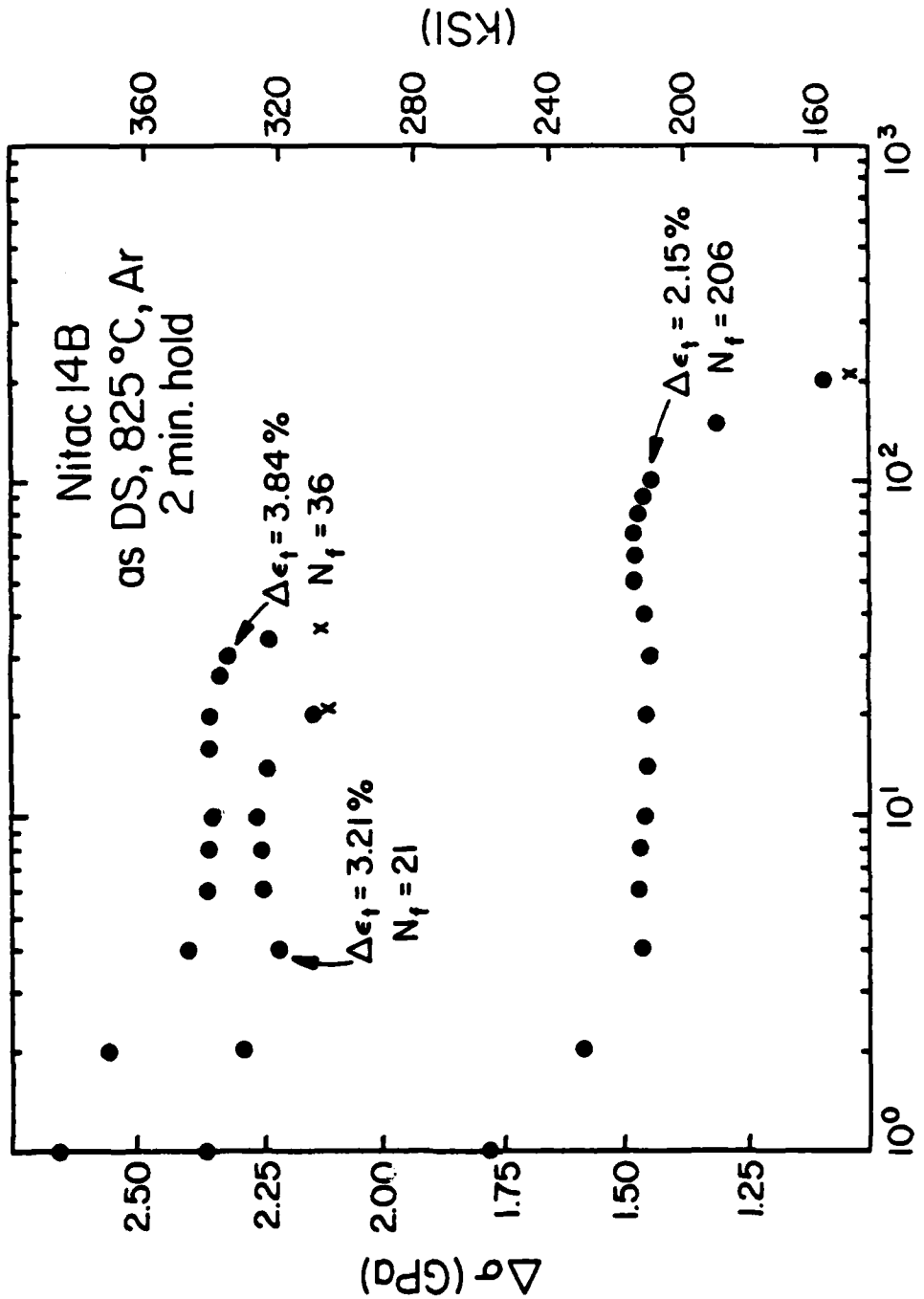

b) 2 min. hole time

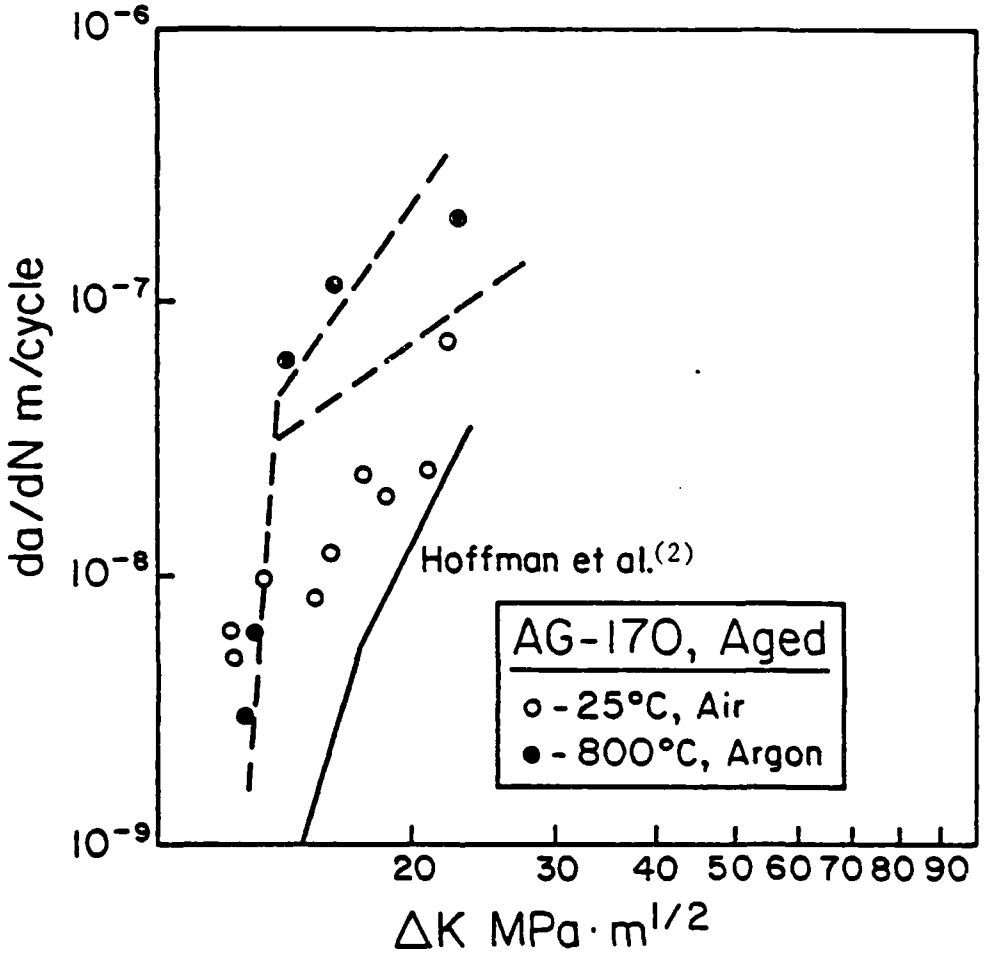

Fig. 13 Effect of temperature on fatigue crack growth of aged AG-170.

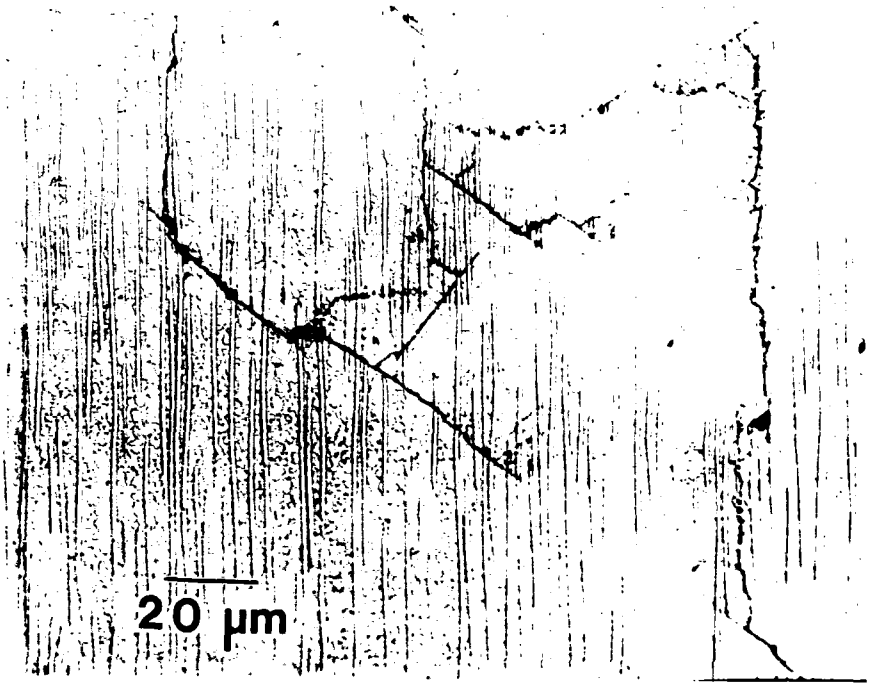

Fig. 14 Crack Branching seen in AG-170, as-D.S., tested at 25°C. Note crystallographic nature.

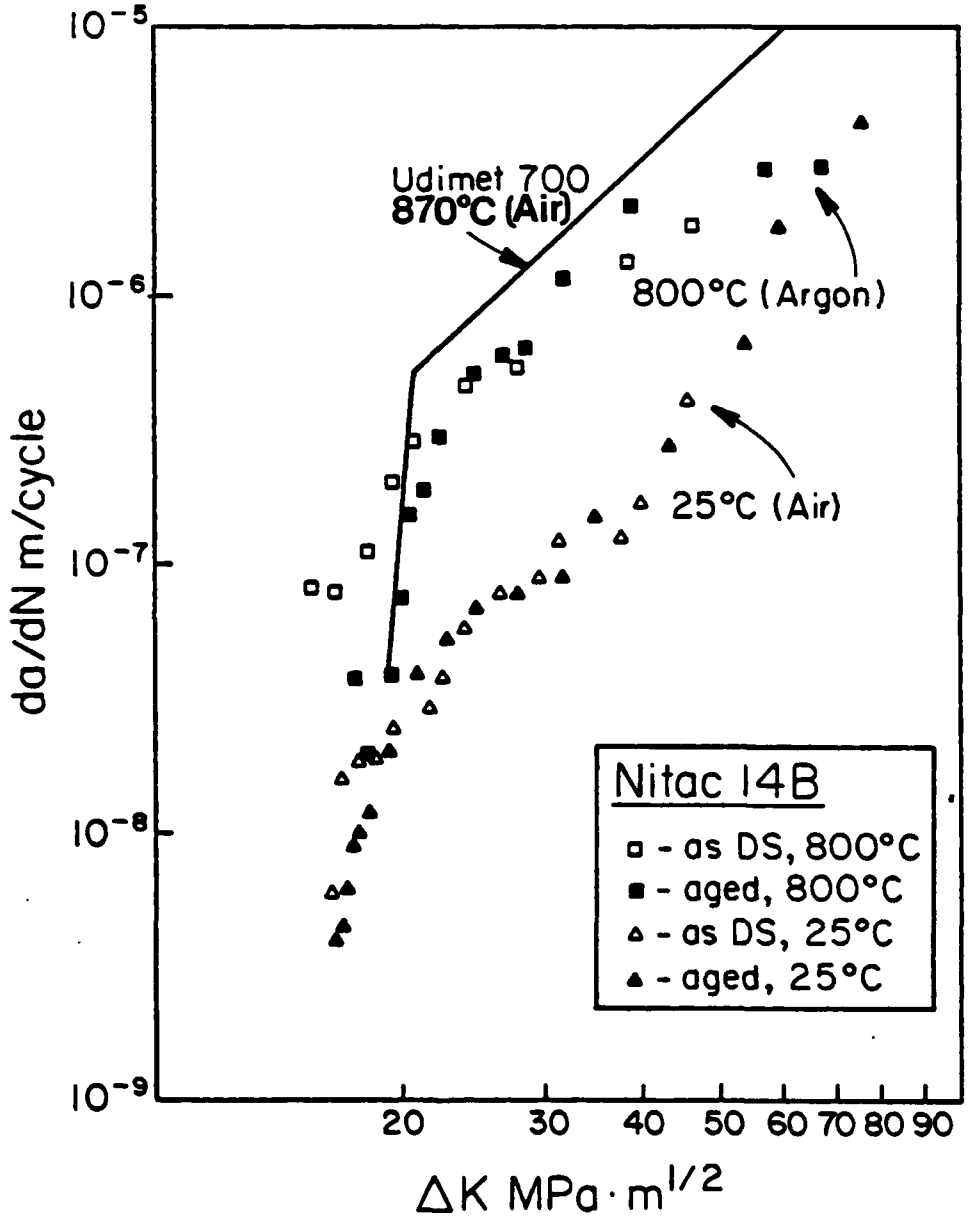

Fig. 15 Effect of temperature on fatigue crack growth of aged and as-D.S. Nitac 14B.

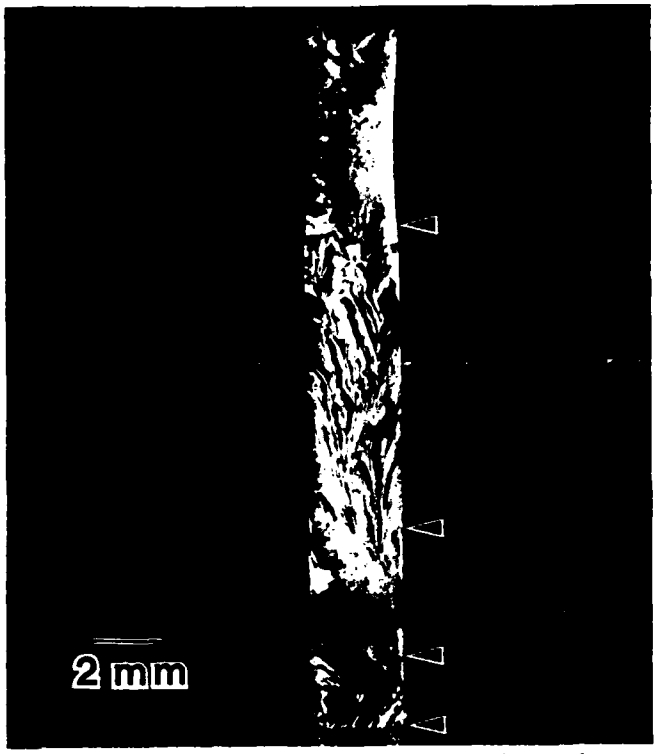

Fig. 16 Macrograph of Nitac 14B, SHT and aged tested at room temperature. Arrows separate distinct fracture regions.

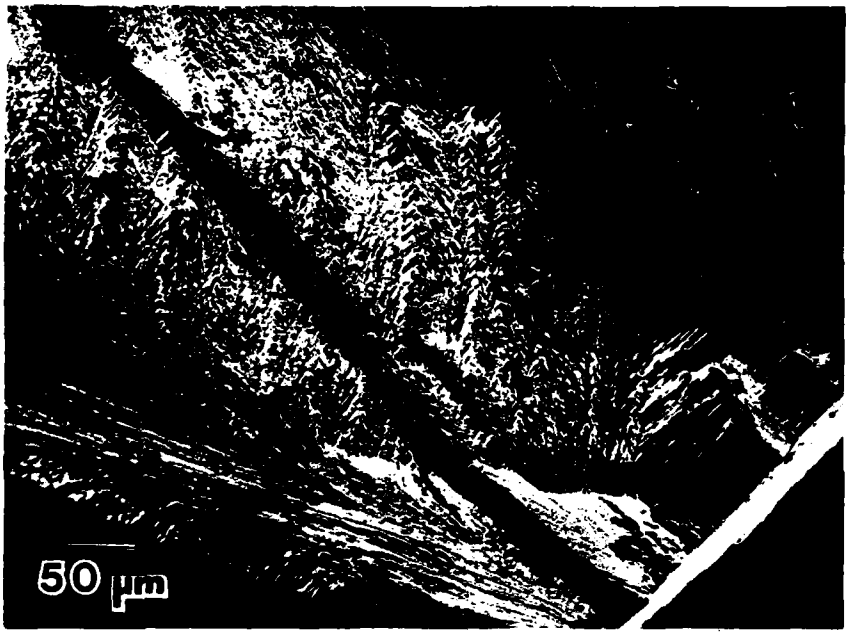

Fig. 17 Initiation region of Stage I cracking in Nitac 14B, as-D.S. tested at room temperature.

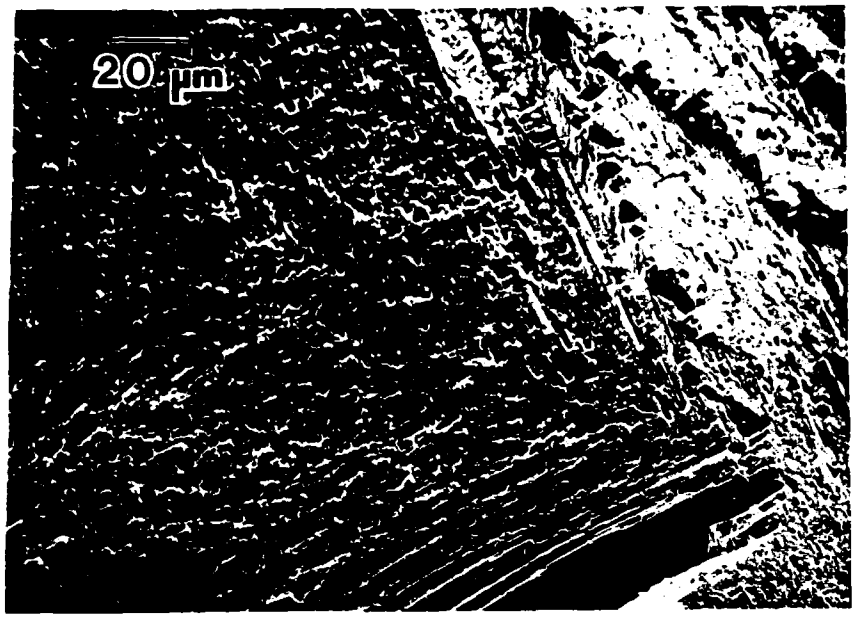

Fig. 18 Transition region from Stage I to fibrous Stage II in Nitac 14B as-D.S. tested at RT. Arrow denotes direction of crack growth.

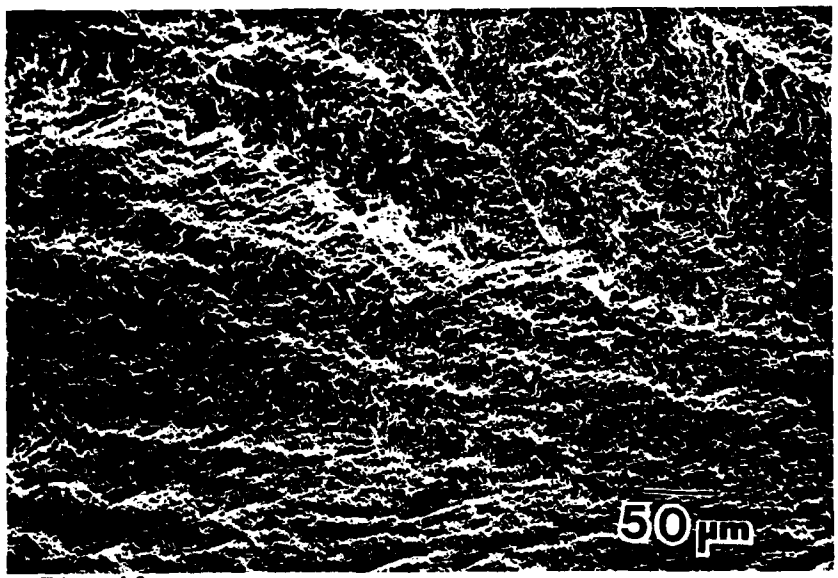

Fig. 19 Feathery and textured Stage II region in Nitac 14B as-D.S. tested at RT.

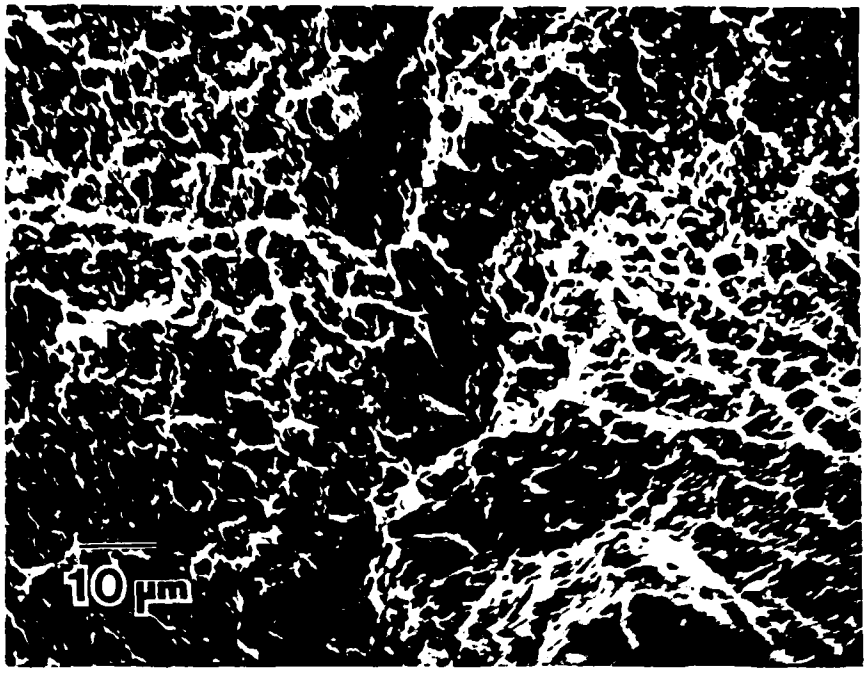

Fig. 20 Dimpled appearance of fatigue zone of Nitac 14B, as-D.S. tested at 800°C.

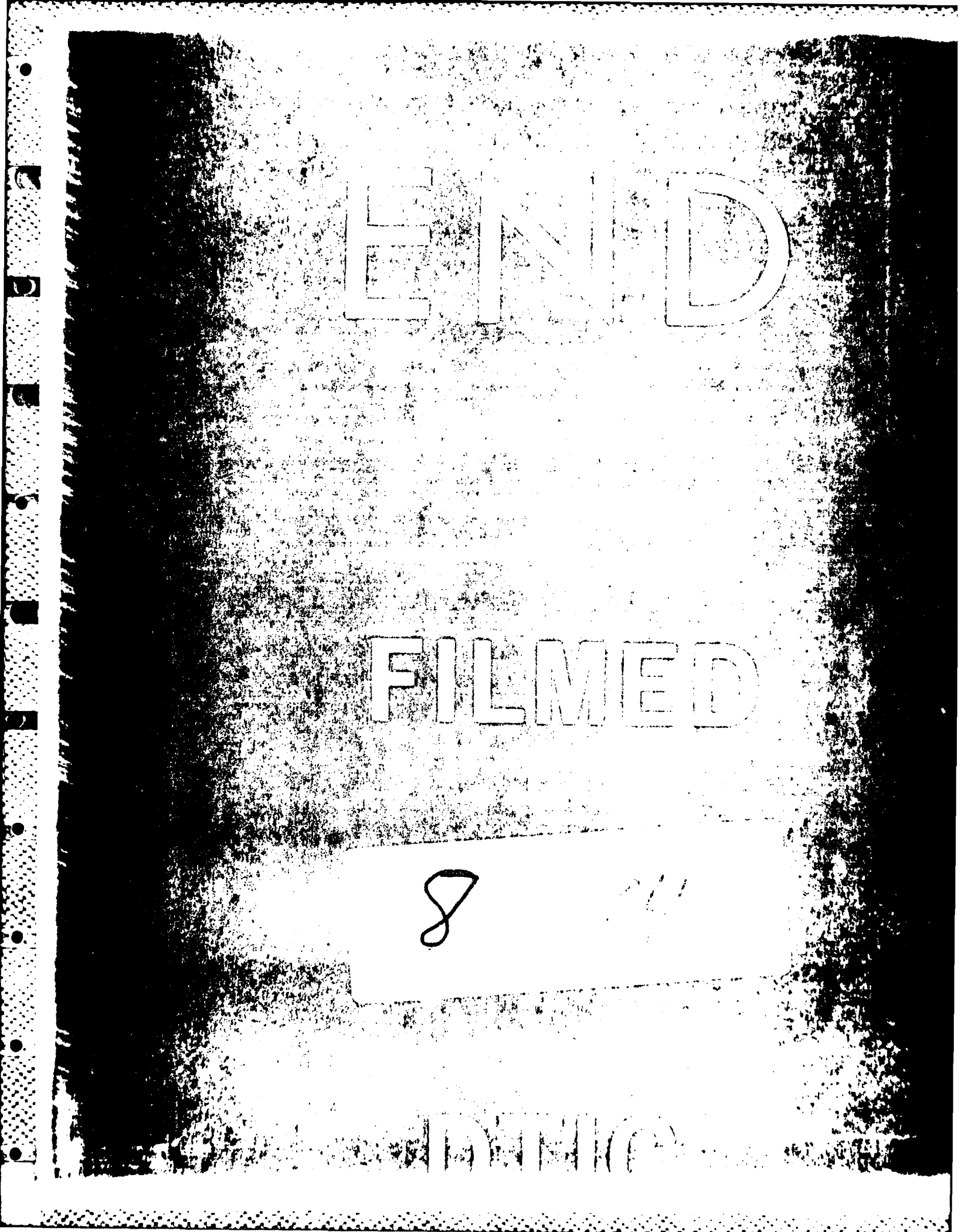
END
FILMED
8